

Structural health monitoring by extraction of coherent guided waves from diffuse fields

Karim G. Sabra

*School of Mechanical Engineering, Georgia Institute of Technology, Atlanta, Georgia 30332-0405, USA
karim.sabra@me.gatech.edu.*

Ankit Srivastava, Francesco Lanza di Scalea, and Ivan Bartoli

*NDE & SHM Laboratory, Department of Structural Engineering,
University of California, San Diego, La Jolla, California 92093-0085, USA
ansrivast@ucsd.edu; flanza@ucsd.edu; ibartoli@ucsd.edu*

Piervincenzo Rizzo

*Department of Civil and Environmental Engineering, University of Pittsburgh, Pittsburgh, Pennsylvania 15260, USA
prizzo@engr.pitt.edu.*

Stephane Conti

*Marine Physical Laboratory, Scripps Institution of Oceanography, La Jolla, California 92037, USA
sconti@ucsd.edu.*

Abstract: Recent theoretical and experimental studies in a wide range of applications have demonstrated that Green's functions (impulse responses) can be extracted from cross-correlation of diffuse fields using only passive sensors. This letter demonstrates the passive-only reconstruction of coherent Lamb waves (dc–500 kHz) in an aluminum plate of thickness comparable to aircraft fuselage and wing panels. It is further shown that the passively reconstructed waves are sensitive to the presence of damage in the plate as it would be expected in a typical “active” guided wave test. This proof-of-principle study suggests the potential for a structural health monitoring method for aircraft panels based on passive ultrasound imaging reconstructed from diffuse fields.

© 2008 Acoustical Society of America

PACS numbers: 43.40.Le, 43.40.Sk, 43.40.Hb, 43.35.Zc [JGM]

Date Received: September 5, 2007 **Date Accepted:** October 30, 2007

1. Introduction

Effective structural health monitoring (SHM) techniques able to detect, locate and quantify damage are needed to ensure the proper performance and maintenance of current and future structures. SHM methods based on ultrasonic guided stress waves are particularly suitable for probing components with waveguide geometries, such as the skin panels of aircraft fuselage and wings (Rose, 1999; Giurgiutiu *et al.*, 2004; Lanza di Scalea *et al.*, 2007).

Guided-wave SHM is traditionally performed in one of two ways: an “active” approach involving at least a source and a receiver, or a “passive” approach involving only receivers. The two approaches offer complementary performances in terms of damage detectability: while the active version is used to detect existing defects in a postmortem mode, the passive version is a mode of acoustic emission monitoring where defects are detected as they grow in real time.

Diffuse, apparently incoherent fields in structures are generally considered “noise,” and would be discarded in conventional SHM. However, from the long-time average of the cross correlation of such noise fields recorded at two sensing points, it is possible to reconstruct the coherent impulse response between the two passive sensors (Sabra *et al.*, 2007). A coherent waveform emerges from noise cross-correlation function (NCF) once the contributions of the diffuse noise sources traveling through both sensors are accumulated over time.

Theoretical and experimental studies have demonstrated the relationship between the Green's function and the NCF for various environments and frequency ranges such as seismology (Shapiro *et al.*, 2005; Sabra *et al.*, 2005c), underwater acoustics (Sabra *et al.*, 2005a, 2005b), civil engineering (Farrar and James 1997; Snieder and Cafak, 2006), low-frequency (<5 kHz) modal properties identification of hydrofoils (Sabra *et al.*, 2007) and ultrasonics (Weaver and Lobkis 2001; Larose *et al.*, 2006; Van Wijk, 2006).

The effects of attenuation and the spatio-temporal statistics of the noise sources often cause the amplitudes of the extracted coherent waveforms of the NCF to differ from those of the theoretical impulse response (Sabra *et al.*, 2005a; Roux *et al.*, 2005; Snieder, 2007). However, Larose *et al.* (2006) were able to image the reflections from a cylindrical hole drilled through an aluminum block using Rayleigh and bulk shear waves which were reconstructed passively. Indeed multiple scattering (e.g., due to a physical boundary or distributed scatterers) typically helps in achieving a fully diffuse wavefield, and thus providing a better estimate of the impulse response (Paul *et al.*, 2005; Larose *et al.*, 2006; Snieder, 2007). A detailed analysis of the role of multiple scattering on the accuracy of the passive imaging technique remains an open question.

This letter shows that passive-only guided-wave SHM can be achieved in a multiply scattering aluminum plate of thickness comparable to an aircraft panel. The passive reconstruction of coherent waves from diffuse fields retains the advantages of the active guided-wave monitoring without a controlled source. The potential could thus exist for passive ultrasound imaging of the aircraft fuselage and wings by exploiting the diffuse vibrations generated by flow unsteadiness during flight (vortices, turbulence) and/or by scattered wavefields (e.g., due to rivets, stiffeners or other structural details).

2. Theoretical background on coherent wave reconstruction from diffuse fields

The expected value of the temporal NCF between two sensors, $C_{12}(t)$, can be computed from the long-time cross correlation of the field $S_1(t)$ measured by sensor 1, and the field $S_2(t)$ measured by sensor 2

$$C_{12}(t) = \int_0^T S_1(\tau)S_2(\tau+t)d\tau, \quad (1)$$

where T is the observation period.

Although defined here in terms of a single temporal integration, the NCF may also be constructed from an ensemble average of shorter duration time averages. The existence of a fully diffuse ambient noise field in the structure is key for the implementation of the passive guided-wave SHM (see, for instance, Weaver and Lobkis, 2004, for further discussions on diffuse field characteristics). This condition ensures the uniform spatial and temporal distribution of the noise sources so that all propagation paths between the two sensors are fully illuminated. In this case, the formal relationship between the Fourier transform of the Green's function between the two sensors, $\tilde{G}_{12}(\omega)$, and the expected value of the Fourier transform of the NCF, $\tilde{C}_{12}(\omega)$, can be expressed as

$$\langle \tilde{C}_{12}(\omega) \rangle = i\beta(\tilde{G}_{12}(\omega) - \tilde{G}_{21}^*(\omega)) \quad (2)$$

where $\langle \rangle$ stands for ensemble average and $*$ stands for complex conjugate. The constant β is related to the power spectrum of the noise excitation, the nature of the recorded signals and the propagation medium. Thus, for a fully diffuse noise field, the NCF is a symmetric function of time. The energy equipartition of the diffuse field is a necessary and sufficient condition to extract the full Green's function from the NCF.

3. Experimental results

Extraction of Lamb coherent waves from diffuse fields was performed on a simple aluminum plate, 1.58 mm (1/16 in.) in thickness (Fig. 1(a)). The excitation was provided by multiple

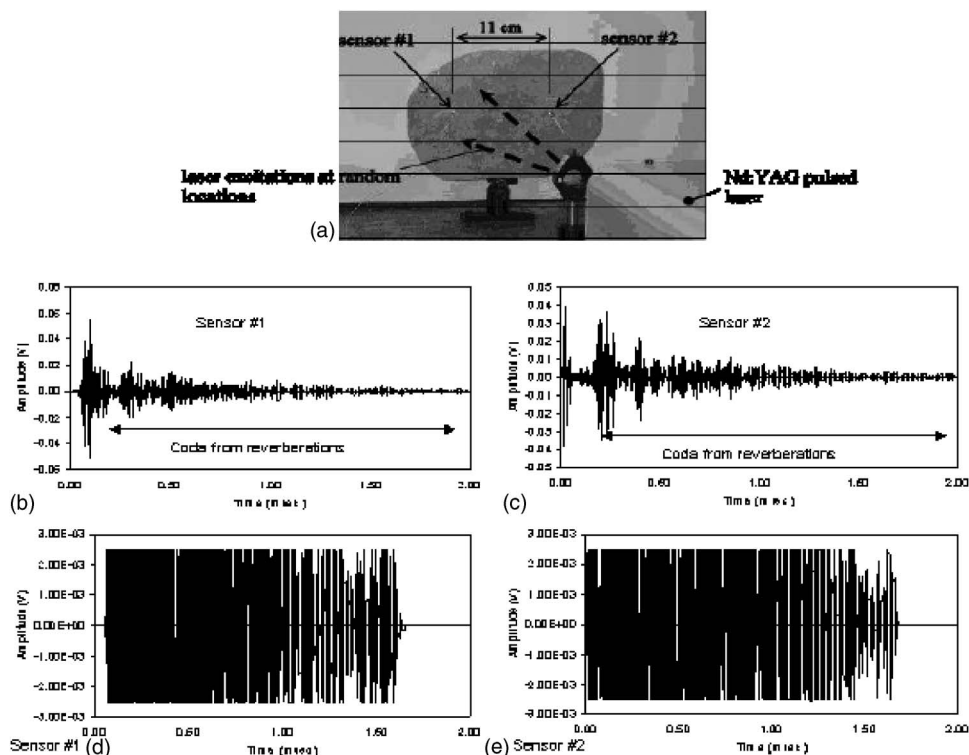


Fig. 1. Experiment on reconstructions of coherent Lamb waves from diffuse fields. (a) A 1.58-mm-thick aluminum plate subjected to random pulsed laser excitation. Plate edges were cut irregularly to randomize the field through multiple reverberations. (b), (c) Raw signals collected by the two sensors following a typical laser excitation showing long coda resulting from reverberations. (d), (e) Same waveforms as (b), (c) but clipped to same level equal to seven times the standard deviation of the electronic noise.

broadband irradiations from an Nd:yttrium—aluminum—garnet pulsed laser (~ 10 ns pulse duration at 1064 nm). The edges of the plate were cut at irregular geometries with no symmetries to produce multiple reverberations and chaotic trajectories of the pulsed excitation to generate diffuse fields. Two commercial acoustic emission sensors (PICO model, Physical Acoustics Corporation, broadband response between 100 kHz and 1 MHz), sensitive to out-of-plane displacements, were spaced 11 cm apart.

Shown in Figs. 1(b) and 1(c) are typical waveforms collected by the two sensors following one laser excitation. The data clearly show a long “coda” which is caused by the reverberating field. Cross correlation was then performed on the coda signals after signal processing involving an amplitude thresholding to assign uniform weights to the multiple reverberations (Larose *et al.*, 2006; Sabra *et al.*, 2007). Figures 1(d) and 1(e) represent the same waveforms shown in Figs. 1(b) and 1(c) where the amplitude was clipped to a same level threshold approximately equal to seven times the standard deviation of the electronic noise level. The data were further randomized by averaging the cross-correlation results obtained from 50 distinct laser excitations aimed at different locations in the plate. The averaged cross-correlation results are shown in Fig. 2(a) for a low-frequency band (dc–15 kHz) and in Fig. 2(b) for a high-frequency band (330–480 kHz).

The theoretical impulse responses relating out-of-plane excitation at sensor 1 to out-of-plane displacements at sensor 2 are also shown for comparison with the reconstructed waves in Figs. 2(c) and 2(d). The predicted Green’s functions were obtained by calculating the forced solutions in the plate using a semianalytical finite element (SAFE) model in the two frequency

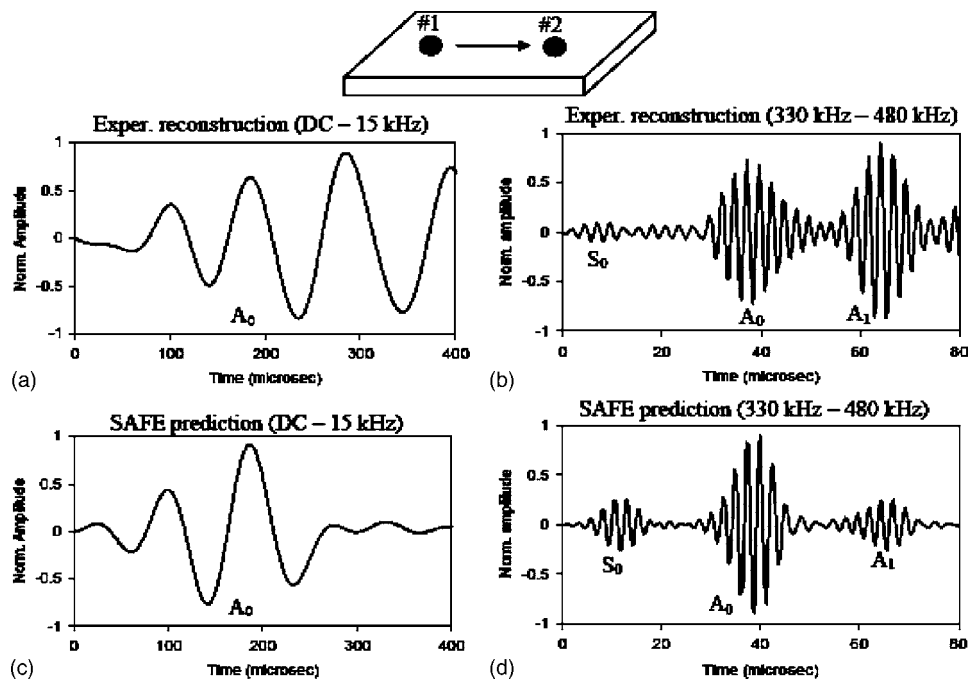


Fig. 2. Reconstruction of coherent guided waves between two sensors in the aluminum plate subjected to random laser excitation. (a) Wave reconstruction in the dc–15 kHz frequency range; (c) corresponding SAFE prediction of out-of-plane Green's function; (b) wave reconstruction in the 330–480 kHz frequency range; (d) corresponding SAFE prediction of out-of-plane Green's function. Notice agreement in arrival times and phase between reconstructed and predicted waves.

bands of interest. These solutions were obtained from Fourier synthesis of the forced harmonic solutions for a point load at the required sensor distance (Hayashi *et al.*, 2003). The computed responses were further convolved with the frequency response of the sensors which were determined experimentally from the laser broadband excitation.

A good agreement is shown in Fig. 2 in both arrival times and phase content between the experimentally reconstructed responses and the SAFE predicted responses. Notice that the later cycles reconstructed in Fig. 2(a) (dc–15 kHz frequency range) are likely due to edge reflections that are absent in the predictions which considered an infinite plate. Amplitude comparisons are more difficult because they are affected by any difference in sensitivity between the two sensors. The reconstruction in the high-frequency band (330–480 kHz) of Fig. 2(b) successfully extracts both A_0 and A_1 modes, again in good agreement with the predictions of Fig. 2(d). The faster S_0 mode is not extracted as efficiently, although it is still discernable. This is associated with the mode shapes of the symmetric mode, which, in the frequency band considered, have large in-plane cross-sectional displacement and small out-of-plane cross-sectional displacement. Overall, Fig. 2 demonstrates that an estimate of the structural impulse response between the two sensors can be obtained passively from the time derivative of the NCF without the use of an active source.

A second set of experiments was conducted to verify that the reconstructed coherent waveforms were suitable for defect detection in the same aluminum plate. A 6.35 mm (1/4 in.)-diam hole was drilled in the plate between sensor 1 and sensor 2, now spaced 18 cm apart (Fig. 3(a)). Figure 3(b) shows the waveforms reconstructed from the random laser excitations in the frequency band 80–160 kHz. The reconstructions are shown for the case of pristine plate, half-thickness hole, and through-thickness hole. As a result of wave scattering, the reductions of amplitude, with respect to the pristine plate case, were, respectively, 22% (half-

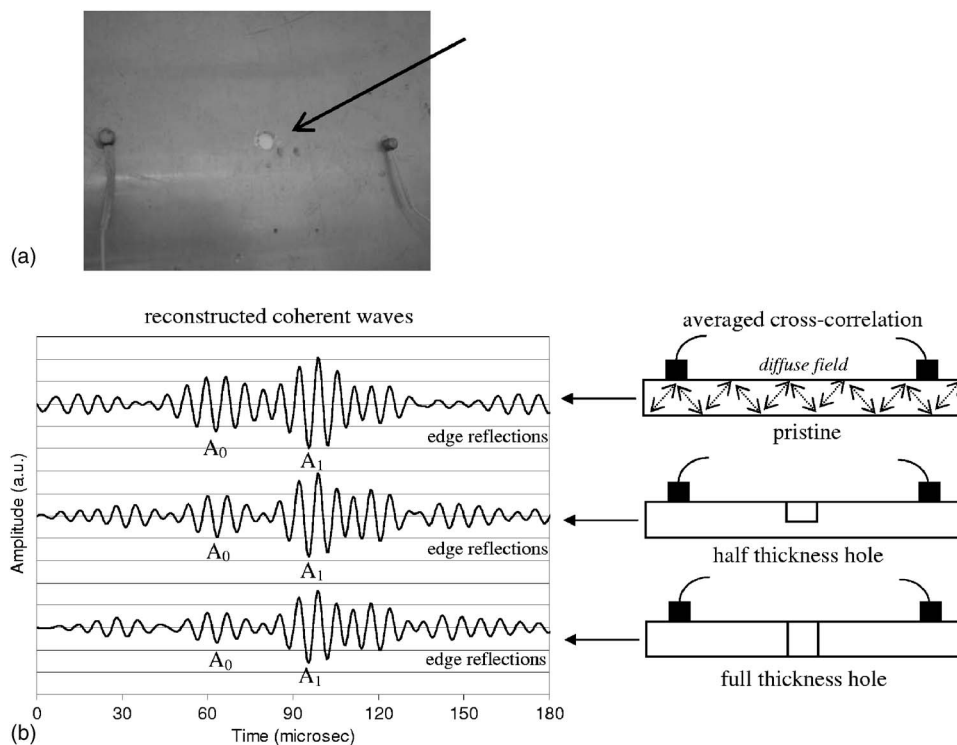


Fig. 3. (a) Picture of hole in test aluminum plate. (b) Coherent waves (80–160 kHz band) reconstructed from random laser excitations of the plate for the case of pristine conditions, 6.35-mm-diam hole extending for half the thickness, and 6.35-mm-diam hole extending through the thickness. Notice the reduction in amplitude of modes S_0 and A_0 caused by wave scattering at the hole. The weak arrival in the $[0-30 \mu\text{s}]$ interval is due to the mode S_0 .

thickness hole) and 40% (through-thickness hole) for the mode A_0 , and similarly 8% and 18% for mode A_1 . The weak arrival in the $[0-30 \mu\text{s}]$ interval is due to the mode S_0 (see Fig. 2). The root-mean-square value (measured at long time $t > 4 \text{ ms}$) of these coherent signals (i.e., “noise level”)—for all three-plate conditions—was equal to 2.5% of mode A_1 amplitude for the pristine case. These values illustrate the fact that not only can the arrival-time structure of the NCF be used for guided-wave SHM but also the NCF’s amplitude information.

4. Conclusions

The extraction of Green’s functions in a structure by the cross-correlation of random noise provides the possibility of active SHM with none, or a limited number of, ultrasonic secondary sources generating a diffuse field. The method was here shown to have the potential for damage detection in a plate-like structure. The Green’s function thus extracted was compared to theoretical predictions, and satisfactory conformance was found in the arrival times and phases of Lamb modes. It was also shown that the reconstructed responses are sensitive to damage in the plate.

Aircraft fuselage and wing structures lend themselves to the formation of diffuse fields because they are geometrically complex (rivets, holes and stiffeners causing scattering) and naturally subjected to random excitations in flight. Furthermore, in order to monitor structural “hot-spots” within the wing structure, it may be more practical to only embed passive sensors during the manufacturing process as opposed to actuators. The diffuse fields in the vicinity of the sensors could also be generated remotely by exciting the outer part of the wing structure during maintenance operations with a few controlled ultrasonic sources strategically located. Hence it is worth investigating the potential for passive-only ultrasonic imaging of these structures during operation.

Acknowledgments

This project was funded in part by Air Force Office of Scientific Research Contract No. FA9550-07-1-0016 (Dr. Victor Giurgiutiu, Program Manager) and by the 2006 Research Fellowship Award from the American Society for Nondestructive Testing.

References and links

- Farrar, C., and James, G. (1997). "System identification from ambient vibration measurements on a bridge," *J. Sound Vib.* **205**, 1–18.
- Giurgiutiu, V., Zagari, A., and Bao, J. (2004). "Damage identification in aging aircraft structures with piezoelectric waver active sensors," *J. Intell. Mater. Syst. Struct.* **15**, 673–687.
- Hayashi, T., Song, W. J., and Rose, J. L. (2003). "Guided wave dispersion curves for a bar with an arbitrary cross section, a rod and rail example," *Ultrasonics* **41**, 175–183.
- Lanza di Scalea, F., Matt, H., Bartoli, I., Coccia, S., Park, G., and Farrar, C. (2007). "Health monitoring of UAV wing skin-to-spar joints using guided waves and macro fiber composite transducers," *J. Intell. Mater. Syst. Struct.* **18**, 373–388.
- Larose, E., Lobkis, O. I., and Weaver, R. L. (2006). "Passive correlation imaging of a buried scatterer," *J. Acoust. Soc. Am.* **119**, 3549–3552.
- Paul, A., Campillo, M., Margerin, L., Larose, E., and Derode, A. (2005). "Empirical synthesis of time-asymmetrical Green functions from the correlation of coda waves," *J. Geophys. Res.* **110**, L003521.
- Rose, J. L. (1999). *Ultrasonic Waves in Solid Media* (Cambridge University Press, Cambridge, U.K).
- Roux, P., Sabra, K. G., Kuperman, W., and Roux, A. (2005). "Ambient noise cross correlation in free space: Theoretical approach," *J. Acoust. Soc. Am.* **117**, 79–84.
- Sabra, K. G., Roux, P., and Kuperman, W. A. (2005a). "Arrival-time structure of the time-averaged ambient noise cross-correlation function in an oceanic waveguide," *J. Acoust. Soc. Am.* **117**, 164–174.
- Sabra, K. G., Roux, P., and Kuperman, W. A. (2005b). "Emergence rate of the time domain Green's function from the ambient noise cross correlation," *J. Acoust. Soc. Am.* **118**, 3524–3531.
- Sabra, K. G., Gerstoft, P., Roux, P., Kuperman, W. A., and Fehler, M. C. (2005c). "Surface wave tomography from microseisms in Southern California," *Geophys. Res. Lett.* **32**, L14311.
- Sabra, K. G., Winkel, E. S., Bourgoyne, D. A., Elbing, B. R., Ceccio, S. L., Perlin, M., and Dowling, D. R. (2007). "On using cross-correlation of turbulent flow-induced ambient vibrations to estimate the structural impulse response. Application to structural health monitoring," *J. Acoust. Soc. Am.* **121**, 1987–2005.
- Shapiro, N. M., Campillo, M., Stehly, L., and Ritzwoller, M. (2005). "High resolution surface-wave tomography from ambient seismic noise," *Science* **29**, 1615–1617.
- Snieder, R., and Cafak, E. (2006). "Extracting the building response using seismic interferometry; theory and application to the Millikan Library in Pasadena, California," *Bull. Seismol. Soc. Am.* **96**, 586–598.
- Snieder, R. (2007). "Extracting the Green's function of attenuating heterogeneous media from uncorrelated waves," *J. Acoust. Soc. Am.* **121**, 2637–2643.
- Van Wijk, K. (2006). "On estimating the impulse response between receivers in a controlled ultrasonic model," *Geophysics* **71**, SI79–SI84.
- Weaver, R. L., and Lobkis, O. I. (2001). "Ultrasonics without a source: Thermal fluctuation correlations at MHz frequencies," *Phys. Rev. Lett.* **87**, L134301.
- Weaver, R. L., and Lobkis, O. I. (2004). "Diffuse fields in open systems and the emergence of the Green's function," *J. Acoust. Soc. Am.* **116**, 2731–2734.